
NOVEL MODELS FOR MULTIPLE DEPENDENT HETEROSKEDASTIC TIME SERIES

A PREPRINT

✉ **Fangyijie Wang**

School of Mathematics and Statistics
University College Dublin
fangyijie.wang@ucdconnect.ie

✉ **Michael Salter-Townshend**

School of Mathematics and Statistics
University College Dublin
michael.salter-townshend@ucd.ie

October 30, 2023

ABSTRACT

Functional magnetic resonance imaging or functional MRI (fMRI) is a very popular tool used for differing brain regions by measuring brain activity. It is affected by physiological noise, such as head and brain movement in the scanner from breathing, heart beats, or the subject fidgeting. The purpose of this paper is to propose a novel approach to handling fMRI data for infants with high volatility caused by sudden head movements. Another purpose is to evaluate the volatility modelling performance of multiple dependent fMRI time series data. The models examined in this paper are AR and GARCH and the modelling performance is evaluated by several statistical performance measures. The conclusions of this paper are that multiple dependent fMRI series data can be fitted with AR + GARCH model if the multiple fMRI data have many sudden head movements. The GARCH model can capture the shared volatility clustering caused by head movements across brain regions. However, the multiple fMRI data without many head movements have fitted AR + GARCH model with different performance. The conclusions are supported by statistical tests and measures. This paper highlights the difference between the proposed approach from traditional approaches when estimating model parameters and modelling conditional variances on multiple dependent time series. In the future, the proposed approach can be applied to other research fields, such as financial economics, and signal processing. Code is available at <https://github.com/13204942/STAT40710>.

Keywords Signal processing · functional MRI · Time series · ARIMA-GARCH model

1 Introduction

In the statistical analysis of time series, the ARMA model describes stationary stochastic process with two polynomials, one is autoregression (AR), and the other one is moving average (MA) Moran [2018]. The GARCH model describes the conditional variance of the current error term related to the squares of previous innovations. Since such a model is used to model time series that exhibit volatility clustering across time Corbyn [2011] and forecast variances across time, the family of GARCH models has been widely developed Bollerslev [1986].

In recent years, many researchers have achieved outstanding performance in applications of ARMA and GARCH models in different research fields, e.g., forecasting stock index by applying ARIMA + GARCH models in 2021 Zolfaghari and Gholami [2021]; obtaining corresponding fluctuation characteristics and forecasting transport flow by ARIMA + GARCH models Lin and Huang [2021]; and so on.

In neural science, researchers are interested in differing intrinsic timescales of brain regions. Takuya Ito used the autocorrelation (AR) function to perform the analysis Ito et al. [2020]. John Fallon characterised BOLD signal dynamics by comparing over 6,000 neural activity time series data. Typically, the fMRI data in different brain regions are modelled with AR(u) or an ARMA(1, 1) process Purdon et al. [2001]. However, the BOLD signal variability is sensitive to age differences and cognitive function Grady and Garrett [2014]. In terms of analysing infants' brain fMRI data, similar technique approaches are still applied. Certainly, some challenges cannot be ignored as they are specific to

infants' brain fMRI studies. Thus, more novel technical approaches are required to be proposed. One obvious challenge is motion. In general, head movement presents a substantial challenge to fMRI research. Infants tend to squirm and hard to stay still, which results in that head movement becoming problematic in infants. As a result, the infants' brain fMRI data shows a presence of sudden timescale volatility. Nevertheless, few studies have directly explored the relationship between timescale volatility in infants' different brain regions. Therefore, this research project focuses on differing and modelling the dependent volatility clustering across different brain regions by examining heteroscedasticity arising from head motion.

Many researchers have performed statistical approaches and model ARMA + GARCH for analysing time-varying variances and correlations primarily in financial time series analysis. This is because economic time series has the unique features of volatility clustering and limitations of using ARMA models. The novel aspect of this research project is adapting such approaches to differing volatility in fMRI data for infants.

This research project is concerned with the statistical analysis of functional magnetic resonance imaging (fMRI) time series data for infants. Functional MRI is widely used to measure brain activity. The technology behind it relies on the theory that blood flows increase in the area of the human brain which is in use Logothetis et al. [2001]. A common method to perform fMRI data is blood oxygenation level- dependent (BOLD). The reason is that neural activity triggers changes in brain blood volume, flow, and oxygenation. However, this mechanism is not fully understood Logothetis [2002]. The fMRI data can be coded as a set of time series. Each time series contains observed BOLD signal variation for a single voxel (a unit representing the signal in brain scans on a three-dimensional grid) with the same time points acquired in a single session. A single voxel represents a tiny cube of brain tissue that can consist of a million brain cells. The researchers can perform statistical analysis of fMRI data to determine the signals induced by neural activity and noise. The BOLD signal observed in the measured signal is used to infer task-related activations in specific brain regions. Many studies have successfully captured task- evoked neural response patterns identified as associated with cognitive processes in brain regions Kanwisher et al. [1997], Haxby et al. [2001].

Because the BOLD signal in the brain is sensitive to fluctuations non-neuronal activity, the head motion has significant, systematic effects on fMRI network measures. Different levels of head motion cause a difference in BOLD signal that could be considered neuronal activity by mistake Van Dijk et al. [2012]. Typically, the fMRI data can be modelled by using the time series Autoregressive model AR (u) or Autoregressive–moving-average model ARMA (u, v). Note that infants tend to move more than adults when they have fMRI scans for the brain, resulting in sudden volatility of infants' fMRI data over time. However, few studies perform statistical analysis on this type of time series data.

This research studies modelling problems for a cluster of associated time series data sets with shared volatility over time. The proposed novel statistical approach fits the model by infant's fMRI time series data of voxels. The research is challenging as it aims to build up multiple complex models constructed of independent AR(u) models and one shared Generalized Autoregressive Conditional Heteroskedasticity GARCH (p, q) model. Equivalently, the white noise term of each AR (u) model is modelled by the same GARCH (p, q) model. No published studies show abilities to successfully identify the correct orders of AR + GARCH and estimate the model parameters. Therefore, the main concern in this research includes model identification, model diagnostics and parameter estimation for the multiple associated models ARMA (u, v) + GARCH (p, q).

Many Neural Sciences researchers will benefit from this research since they have shown high interest in measuring the activity of different brain regions by exploring fMRI data Ito et al. [2020]. Moreover, the novel approach is extended to modelling finance time series data with sudden volatility caused by exogenous shocks, e.g., company share value. The researchers can adapt this novel approach to perform statistical analysis of complex nonlinear data with volatility in various research fields.

2 Theory

2.1 ARMA time series models

If a series is partly autoregressive and partly moving average, then it is a general time series model. It can be named a mixed autoregressive moving average model of orders p and q , ARMA(p, q). It is generally represented as below equation Corbyn [2011]:

$$Y_t = \phi_1 Y_{t-1} + \phi_2 Y_{t-2} + \dots + \phi_p Y_{t-p} + e_t - \theta_1 e_{t-1} - \theta_2 e_{t-2} - \dots - \theta_q e_{t-q} \quad (1)$$

For the general ARMA(p, q) model, the condition of stationary is $|\phi| < 1$ Corbyn [2011]. To identify the value of p and q , the sample autocorrelation function (ACF) in Equation 2 and the partial autocorrelation function (PACF) in Equation

	AR(p)	MA(a)	ARMA(p, q), $p > 0$, and $q > 0$
ACF	Tails off	Null after lag q	Tails off
PACF	Null after lag p	Tails off	Tails off

Table 1: The summary of ACF and PACF behaviours for different time series models

3 is applied Corbyn [2011]:

$$\rho_k = \frac{\sum_{t=1}^{n-k} (Y_t - \bar{Y})(Y_{t+k} - \bar{Y})}{\sum_{t=1}^n (Y_t - \bar{Y})^2} \quad k = 1, 2, \dots \quad (2)$$

$$\phi_{k,k} = \frac{\rho_k - \sum_{j=1}^{k-1} \phi_{k-1,j} \rho_{k-j}}{1 - \sum_{j=1}^{k-1} \phi_{k-1,j} \rho_j} \quad j = 1, 2, \dots, k-1 \quad (3)$$

For ARMA(p, q), to identify p , Quenouille (1949) showed that the following approximation holds Corbyn [2011] for a white noise process:

$$\text{var}(\phi_{k,k}) \approx \frac{1}{n} \quad (4)$$

Thus $\pm 2/n$ is the critical limit on $\phi_{k,k}$ to test the null hypothesis that an AR(p) model is correct. If $\phi_{k,k}$ breaks down to 0 for some k , there is evidence for $p = k$. To identify q , $\pm 2/n$ can also be used as the critical limits on ρ_k . The null hypothesis can be rejected if and only if ρ_k exceeds these limits. And it shows evidence for $q = k$.

The sample ACF and PACF are practical visual tools for identifying orders of AR and MA models. But for a mixed ARMA model, the ACF and PACF have infinitely nonzero values. The summary of ACF and PACF behaviours are shown in Table 1. So it is challenging to identify p and q Corbyn [2011]. Although other graphical tools are proposed to support us in identifying p and q , in this project, only AR(p) model or MA(q) model is considered instead of a mixed ARMA(p, q) model. This is due to the invertibility characteristic of the AR and MA model, which is explained in section 2.2.

2.2 Invertibility

An MA (q) can be invertible, which means it can be inverted into an infinite-order AR model. For instance, an MA (1) model is considered as:

$$Y_t = \varepsilon_t - \theta \varepsilon_{t-1} \quad (5)$$

Equation 5 can be rewritten as:

$$\varepsilon_t = Y_t + \theta Y_{t-1} + \theta^2 Y_{t-2} + \dots \quad (6)$$

or

$$Y_t = (-\theta Y_{t-1} - \theta^2 Y_{t-2} - \theta^3 Y_{t-3} - \dots) + \varepsilon_t \quad (7)$$

by continuously replacing t with $t-1$ and substituting for ε_{t-1} when $|\theta| < 1$ Corbyn [2011]. For a general MA (q) or ARMA(p, q) model, if it is invertible, it can be inverted to an AR(p) model with a large p . In this project, the proposed model will only have AR(p) component instead of ARMA(p, q). When p is increased to a large value, the model equivalently has an ARMA(p, q) component.

2.3 Time series model of heteroscedasticity

Consider a single time series data Y_t with high volatility, the conditional variance of Y_t is given by the past Y values, Y_{t-1}, Y_{t-2}, \dots . In practice, the one-step-ahead conditional variance varies with the current and past values. Therefore, the conditional variance is a random process. To study the volatility of a time series, applying the McLeod-Li test Field McLeod and Li [1983] for the presence of volatility is useful. In 1982, Engle first proposed the autoregressive conditional heteroscedasticity (ARCH) model for modelling the changing variance of a time series Engle [1982]. The null hypothesis of the McLeod-Li test is that no autoregressive conditional heteroskedasticity (ARCH) is present among the lags considered. It is computing the squared series data or the squared residuals from an ARMA model and then performing Ljung-Box test LJUNG and BOX [1978] with the calculated results. When there is k out of n p-values significant at the 0.05 significance level among lags n , and $\frac{k}{n} > 0.05$, the null hypothesis is likely to reject.

Another popular model to represent the dynamic evolution of volatility in time series is the Generalized Autoregressive Conditional Heteroscedasticity (GARCH) model Bollerslev [1986].

$$\begin{aligned} Y_t &= \sigma_{t|t-1} \varepsilon_t \\ \sigma_{t|t-1}^2 &= \alpha_0 + \alpha_1 Y_{t-1}^2 + \cdots + \alpha_q Y_{t-q}^2 + \beta_1 \sigma_{t-1|t-2}^2 + \cdots + \beta_p \sigma_{t-p|t-p-1}^2 \\ \varepsilon_t &\sim N(0, 1) \end{aligned} \quad (8)$$

The orders of GARCH are p and q . In Equation 8, the standardized residuals $\hat{\varepsilon}_t$ are computed as $Y_t/\sigma_{t|t-1}$. If the GARCH model is correct, $\hat{\varepsilon}_t$ is independent and identically distributed Corbyn [2011]. To identify p and q in GARCH(p, q), the method examines the ACF and PACF of squared Y_t . If Y_t is following GARCH(p, q), then Y_t^2 is following ARMA($\max(p, q), p$) Corbyn [2011]. However, sometimes it is difficult to identify p and q because of more fluctuation and high variance in data. Some existing well-known Information Criteria, Akaike Information Criteria (AIC), Bayesian Information Criteria (BIC), can help us choose the correct model from a list of candidate GARCH(p, q) models Naik et al. [2020]. The lower AIC or BIC, the candidate GARCH model is better. The AIC value can be calculated from the maximum likelihood estimate of the GARCH model, and it is defined as:

$$AIC = 2K - 2 \ln(L) \quad (9)$$

In Equation 9, K is the number of independent variables used, and L is the log-likelihood estimate of the candidate GARCH model.

3 Methods

This research project will implement the proposed statistical analysis approach in R programming language using the software RStudio.

Initially, a single time series data will be simulated from a model AR(1) + GARCH(1, 1) with fixed orders and model parameters. The simulation time series data will be used for statistical analysis afterwards. The sample Autocorrelation Function (ACF) and the sample Partial Autocorrelation Function (PACF) (Corbyn, 2011) plots provide practical graphical tools for identifying the orders of AR(u) or MA(v) models. Fit the identified AR(u) model to the simulation data, and the squared residuals from this model can be used to test for the presence of ARCH (or GARCH). The McLeod-Li (McLeod and Li, 1983) test can refer to conditional heteroscedasticity (ARCH) effects by using several lags and plotting the p-value of the statistical tests. The GARCH model is an extension of the ARCH model that incorporates a moving average component together with the autoregressive part. The model identification techniques for ARMA models can also be applied to the squared residuals. Plotting ACF and PACF of the squared residuals typically indicates ARMA($\max(p, q), p$) model is the suitable model for the squared residuals Corbyn [2011]. Thus, a GARCH(p, p) model is fitted at first, and then q can be estimated by examining the significance of the resulting ARCH coefficient estimates. After this, a model AR(u) + GARCH(p, q) is fitted to the simulation data to estimate the model parameters ϕ , α , β .

Similarly, the technical approach is applied to multiple dependent heteroskedastic time series. It starts with simulating data from various models with shared volatility clustering across time $y_i = \text{AR}(u_i) + \text{GARCH}(p, q)$ as below:

$$\begin{aligned} y_1 &= \text{AR}(u_1) + \text{GARCH}(p, q) \\ y_2 &= \text{AR}(u_2) + \text{GARCH}(p, q) \\ y_3 &= \text{AR}(u_3) + \text{GARCH}(p, q) \\ &\dots \end{aligned} \quad (10)$$

Then sample ACF and sample PACF are used to identify each AR orders u_i . A collection of AR(u_i) models are fitted to each time series separately. Therefore, a series of estimated residuals $\hat{\eta}_i$ returned from each time series $\{y_i\}$ is obtained. The next step is averaging over all the N series ($\frac{1}{N} \sum_{i=1}^N \hat{\eta}_i$) to obtain the average value of all estimated residuals. Note that the estimated residuals are shared components in all N series. Calculate the average of N estimated residuals $\{\hat{\eta}_t\}$ as $\bar{\hat{\eta}}_t$ and plot ACF and PACF of the $\bar{\hat{\eta}}_t$ so that the GARCH orders can be identified. Equivalently, the model identification techniques for ARMA models are used to identify p and $\max(p, q)$. When fitting the GARCH(p, q) to the average value of N estimated residuals $\{\bar{\hat{\eta}}_t\}$, the estimated coefficients (α_i, β_i) are obtained by maximising the likelihood function of the GARCH model Corbyn [2011].

$$L(\hat{\omega}, \hat{\alpha}, \hat{\beta}) = -\frac{n}{2} \log(2\pi) - \frac{1}{2} \sum_{i=1}^n \left\{ \log \left(\hat{\sigma}_{t|t-1}^2 \right) + \hat{\eta}_t^2 / \left(2\hat{\sigma}_{t|t-1}^2 \right) \right\} \quad (11)$$

There is no closed-form solution for the maximum likelihood estimators of $\hat{\omega}$, $\hat{\alpha}$ and $\hat{\beta}$, but they can be computed numerically. A series of models can be built, including a shared GARCH model plus multiple independent AR(u) models. Afterwards, fitting such a series of models to fMRI data performs the goodness of fit test for the fitted AR + GARCH model.

3.1 Simulate data

The simulation work starts with simple models and fixed parameters. The objectives are simulating multiple time series data sets with given parameters and orders. The simulated data will be used for model fitting and parameter estimation.

The mixed model AR(u) + GARCH(p, q) is proposed. In general, the model is used for modelling multiple dependent series data, so it contains multiple AR + GARCH formulas that can be written as:

$$\begin{aligned} Y_{1t} &= \mu + \sum_{i=1}^u \phi_{1i} Y_{t-i} + \eta_{1t} \\ Y_{2t} &= \mu + \sum_{i=1}^u \phi_{2i} Y_{t-i} + \eta_{2t} \\ &\vdots \\ Y_{kt} &= \mu + \sum_{i=1}^u \phi_{ki} Y_{t-i} + \eta_{kt} \end{aligned} \quad (12)$$

And the squared residuals $\{\eta_{kt}\}$ are shared with each formula. It is assumed that the average of $\{\eta_{kt}\}$, $\bar{\eta}_t$, can be fitted by a GARCH(p, q) model. Thus, its formula is written as:

$$\begin{aligned} \bar{\eta}_t &= \sigma_{t|t-1} \varepsilon_t \\ \sigma_{t|t-1}^2 &= \alpha_0 + \alpha_1 \eta_{t-1}^2 + \cdots + \alpha_q \eta_{t-q}^2 + \beta_1 \sigma_{t-1|t-2}^2 + \cdots + \beta_p \sigma_{t-p|t-p-1}^2 \end{aligned} \quad (13)$$

In the beginning, the orders $\{u, p, q\}$ are given fixed values $\{1, 1, 1\}$. Therefore, the simple model is AR(1) + GARCH(1, 1). The coefficient parameter φ of AR model is given 0.05, close to 0.0. The coefficient parameter $\{\alpha, \beta\}$ of GARCH model are randomly given fixed values $\{0.2, 0.5\}$. In total, 20, 100 and 400 time series data are simulated with this AR(1) + GARCH(1, 1) model. These time series data are used to assess whether the size of the data set impacts the results of parameter estimation.

Afterwards, another AR(1) + GARCH(1, 1) model is created with the parameters as the previous simulation, except parameter φ . The parameter φ of AR model is set as a random number in a range (0.7, 0.9), close to 1.0. This new model is used for simulating 400 time series data sets. Parameter estimation is performed on these data sets. Then the results are compared with previous parameter estimation with 400 time series data with fixed φ . The objective of this simulation work is to assess whether parameter estimation results behave differently when the parameter φ is a fixed value and a random value.

In the end, 400 time series data are simulated with AR(1) + GARCH(1, 1) model. But the first 200 time series have $\alpha = 0.2, \beta = 0.5$, and φ is a random number in range (0.01, 0.05). The reset 200 time series have the same $\{\alpha, \beta\}$ as $\{0.2, 0.5\}$. The only difference is that parameter φ is in the range (0.7, 0.9). These 400 time series data together are used for parameter estimation. The objective is to understand the behaviour of parameter estimation when the parameter φ is close to 0.0 and 1.0.

All simulated time series data contain 300 time points ($N = 300$) as default.

3.2 Model identification and parameter estimation

The following estimation work is programmed in R language using RStudio.

When 20, 100, 400 time series data are simulated, each time series' ACF and PACF values are calculated in a created loop function. (1) Comparing the ACF and PACF among the first 20 lags to count the number of PACF values which are significantly not null ($\pm 2/n$ is the critical limit) when ACF decays exponentially fast. The number of these non-null PACF values k is equal to the AR orders, p . The estimated model is named AR(\hat{p}). If only PACF decays fast, then counting the number of ACF values that are not equal to null. This number k is equal to the MA orders, q , so the estimated model is named MA(q). If ACF and PACF decay fast and exponentially, this is evidence that the ARMA

model is present. But the fixed model ARMA is not considered at the stage of this project. (2) After the estimated AR model is fitted on each series Y_{it} , a set of squared residuals $\{\hat{\eta}_{it}\}$ is returned. Then, compute the average of $\{\hat{\eta}_{it}\}$ for 20, 100 and 400. (3) Afterwards, the ACF and PACF of the averaged $\bar{\eta}_t$ are calculated for identifying GARCH orders p and q . It is the same identification method used for identifying AR orders. The estimated GARCH(p, q) model is fitted on averaged $\bar{\eta}_t$ and model diagnostic is performed afterwards. The goal of the diagnostic is to measure the goodness of fit of the estimated GARCH model. (4) Each series data Y_{it} minus averaged $\bar{\eta}_t$ before calculating ACF and PACF of series again. This step is to identify the AR orders p again and estimate parameter φ_i after each series Y_{it} is fitted by the estimated AR(p) model.

The previous four analysis steps are also executed on the 400 simulated time series data with parameter φ_i in range (0.7, 0.9). (1) Computing ACF and PACF of each series Y_{it} and checking their behaviour to identify the order of the AR model for Y_{it} ($\pm 2/N$ is the critical limit). (2) Once the AR model is fitted on each series, the returned residuals $\{\hat{\eta}_{it}\}$ from each fitted model are collected. (3) The averaged residuals $\bar{\eta}_t$ is computed from the collection of returned residuals $\{\hat{\eta}_{it}\}$. After this, the $\bar{\eta}_t$ is removed from each series Y_{it} and ACF and PACF of $\bar{\eta}_t$ are calculated for identifying orders of GARCH model p and q . The estimated GARCH(p, q) model is fitted on $\bar{\eta}_t$ before performing model diagnostic. (4) Calculating ACF and PACF on each series data Y_{it} to identify orders of the AR model u_i . To estimate coefficient parameters φ_i , it can be retrieved from results of fitting the estimated AR(u_i) model.

The methods used for analysing the mixed 400 simulated time series with variant parameters differ from previous methods. The reason is that some backwards are found when estimating parameters. The details of backwards will be explained in the following few sections. This new analysis methods are described as: (1) The ACF and PACF of series data Y_{it} are computed for the first 20 lags. And they are used for identifying AR orders p and q . Then $\{Y_{it}\}$ is fitted with the estimated ARMA(\hat{p}, \hat{q}) model to get model residuals $\{\hat{\eta}_{it}\}$. Also, the coefficient parameters φ_i are estimated after model fitting. All estimated $\hat{\varphi}_i$ are stored in a numerical vector $\hat{\varphi}_{1i}$ that is used for final estimation later. (2) A weight parameter W_i is calculated by using each estimated $\hat{\varphi}_{1i}$, and it can be written as:

$$\begin{aligned} w_i &= \frac{1}{\hat{\varphi}_{1i}} \\ W_i &= \frac{w_i}{\sum w_i} \end{aligned} \quad (14)$$

Afterwards, the averaged residuals $\bar{\eta}_t$ is calculated by multiplying the weight W_i with each model residuals $\{\hat{\eta}_{it}\}$:

$$\bar{\eta}_t = \sum_{i=1}^K W_i \hat{\eta}_{it} \quad (15)$$

(3) Calculating the ACF and PACF of averaged residuals $\bar{\eta}_t$ is the method used for identifying the orders of GARCH model p and q . An estimated GARCH model can be built with \hat{p} and \hat{q} . The model is fitted on the averaged residuals $\bar{\eta}_t$ so that model diagnostic can be performed. (4) The averaged residuals $\bar{\eta}_t$ is removed from each series Y_{it} . The ACF and PACF of each series $\{Y_{it} - \bar{\eta}_t\}$ are identified to build the estimated ARMA(\hat{p}, \hat{q}). The estimated ARMA models are fitted on each $\{Y_{it} - \bar{\eta}_t\}$ to get the estimated coefficient parameters $\hat{\varphi}_2$. All $\hat{\varphi}_2$ are stored in numerical vector $\hat{\varphi}_{2i}$. (5) Average two numerical vectors $\hat{\varphi}_{1i}$ and $\hat{\varphi}_{2i}$ to get the final estimation of parameter $\hat{\varphi}_i$.

3.3 Fit model on real-world data

The real-world data set is collected from two real fMRI data sets, subject CC110045 and subject CC110056. And subject CC110056 shows high volatility than subject CC110045. Each subject represents the time course for a different area, called Region of Interest (ROI) in the brain. There are 400 ROIs in each subject, and each ROI time series data contains 261 time courses. Typically, ROIs beside each other in the brain have high correlations. Both data sets have no missing values and no invalid numerical values, see Figure 1. They are valid time series data examined by visualisation tools.

The improved analysis method is applied to real-world fMRI data. The estimation of parameters and model fitting are examined statistically. It includes estimated AR orders \hat{p}_i , estimated GARCH orders (\hat{p}, \hat{q}), estimated AR coefficients $\hat{\varphi}_i$, the averaged residuals $\bar{\eta}_t$, and standardized residuals $\hat{\varepsilon}_i$. Especially, to evaluate the new improved method, the coefficients estimator $\hat{\varphi}_i$ is compared to the old coefficients' estimator $\hat{\varphi}_{i_old}$ that are generated from the old statistical analysis method.

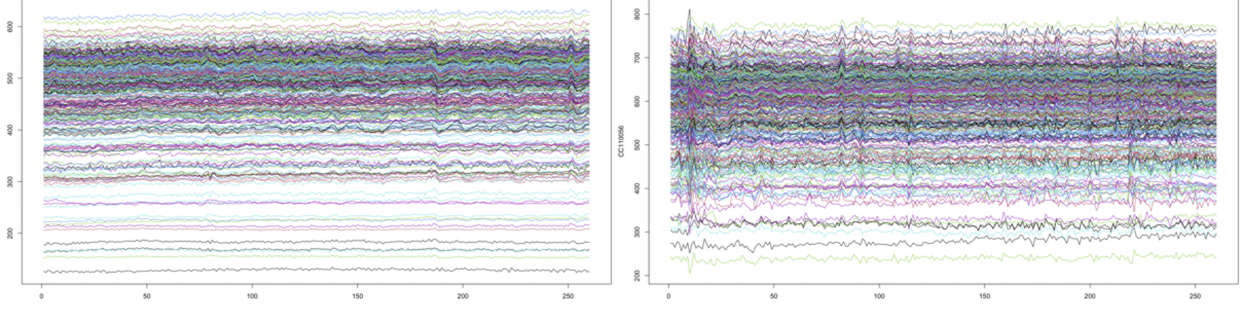
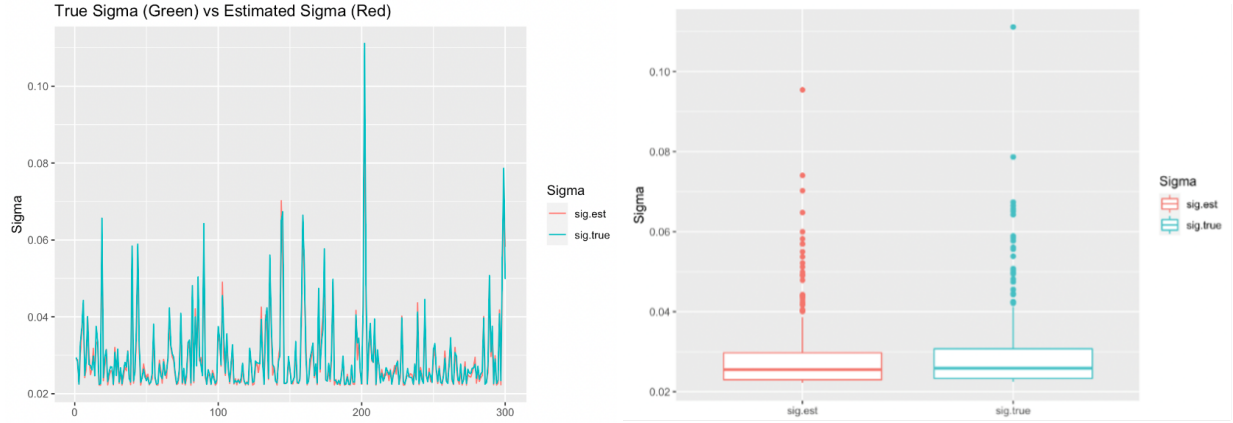


Figure 1: Subject CC110056 shows high volatility on the left. On the right, CC110045 fMRI shows very little movement.



(a) Plots of actual sigma $\sigma_{t|t-1}$ and estimated sigma $\hat{\sigma}_{t|t-1}$ (b) Boxplots of actual sigma $\sigma_{t|t-1}$ and estimated sigma $\hat{\sigma}_{t|t-1}$

Figure 2

4 Results and Discussion

The idea of simulating multiple time series in different scenarios is to help us evaluate the performance of the proposed modelling methods and to understand the behaviour of numerous dependent time series data with volatility. In this section, there are some plots and tables to present the results of the modelling.

In the modelling, there are four critical parameters in consideration and comparison, $\hat{\eta}_t$, $\sigma_{t|t-1}$, ε_t and φ_i . The first parameter $\hat{\eta}_t$ is the averaged value of multiple residuals returned from AR models. It is possible to assess the modelling of $\hat{\eta}_t$ by evaluating the estimation of $\sigma_{t|t-1}$ and returned standardized residuals $\hat{\varepsilon}_t$, because Equation 8 shows that $\hat{\eta}_t$ is determined by the product of $\sigma_{t|t-1}$ and ε_t . As our assumptions state, the distribution of ε_t follows a normal distribution. Thus, the distribution of $\hat{\varepsilon}_t$ is assessed by a normal quantile-quantile plot (Q-Q plot) WILK and GNANADESIKAN [1968]. Comparing the estimated $\hat{\sigma}_{t|t-1}$ to the actual $\sigma_{t|t-1}$ to assess its accuracy of estimation. This method evaluates the estimation of $\sigma_{t|t-1}$ and examines the fitting performance of GARCH model.

Another critical parameter $\hat{\varphi}_i$ is estimated from the fitted AR model. Since the actual values of φ_i are known, its estimation is assessed by computing the mean squared error (MSE) of $\hat{\varphi}_i$. And the scatter plot of $\hat{\varphi}_i$ and φ_i is a visualisation tool to assess the estimation accuracy.

4.1 Simulation study I - Different sizes of data sets

When the parameters are given fixed values and the size of the simulated time series data set increases from 20 to 100, the estimation of $\sigma_{t|t-1}$ can be evaluated by the below plots:

The above plots show that the estimator $\hat{\sigma}_{t|t-1}$ are very close to the actual values of $\sigma_{t|t-1}$. And the mean value of the estimator $\hat{\sigma}_{t|t-1}$ is approximately equal to the expected mean of $\sigma_{t|t-1}$. Also, the plots indicate that the values of estimator $\hat{\sigma}_{t|t-1}$ do not change a lot when the size of the data set is increasing. When the size of data set increases to

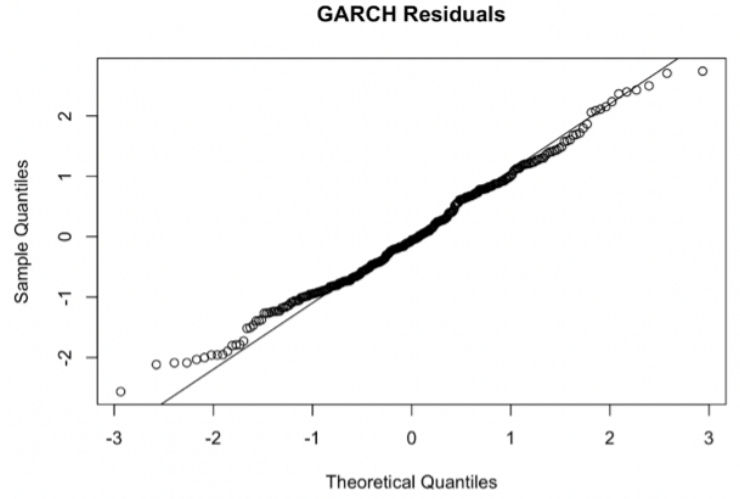


Figure 3: Q-Q plots of actual ε_t and estimated residuals $\hat{\varepsilon}_t$

	GARCH(1, 1)	GARCH(2, 2)
AIC	-0.7293573	-0.7181245

Table 2: Comparison of AIC values between two models

400, the values of estimator $\hat{\sigma}_{t|t-1}$ are still close to the actual values of $\sigma_{t|t-1}$ without significant variance. Thus, the estimation of $\sigma_{t|t-1}$ is quite good.

When the size of data sets increases, the distribution of standard residuals $\hat{\varepsilon}_t$ follows a normal distribution. The Q-Q plots of estimator $\hat{\varepsilon}_t$ are shown in Figure 3:

It also means that the assumption of the proposed model parameter $\hat{\varepsilon}_t$ is correct and accepted. Equivalently, the value of averaged estimator $\bar{\hat{\eta}}_t$ should be good as expected because it is only determined by values of $\hat{\sigma}_{t|t-1}$ and $\hat{\varepsilon}_t$.

Further, the orders of the averaged estimator $\bar{\hat{\eta}}_t$ is consistently identified as (1, 1) when the size of data sets increases from 20 to 400. Table 2 presents that fitting the GARCH(1, 1) model on estimator $\bar{\hat{\eta}}_t$ always returns the lowest AIC using MLE. Although GARCH(2, 2) is fitted on $\bar{\hat{\eta}}_t$, the model GARCH(1, 1) achieves the lowest AIC. Thus, GARCH(1, 1) is considered the best-fit model. After removing $\bar{\hat{\eta}}_t$ from each series, the values of estimator $\hat{\varphi}_l$ varies differently. To compare the actual values to the estimated values, it is necessary to plot values with scatter plots, Figure 4.

When looking at the first plot of φ_i and estimator $\hat{\varphi}_l$, it is clear to see few estimated values larger than the actual value (0.05), and the reset of values are less than 0.05. The estimator mainly underestimates the parameters φ_i . When the size of data sets increases to 400, all estimator values $\hat{\varphi}_l$ are less than the actual value (0.05). Referring to these plots, the estimation of φ_i is biased when the size of data sets is large.

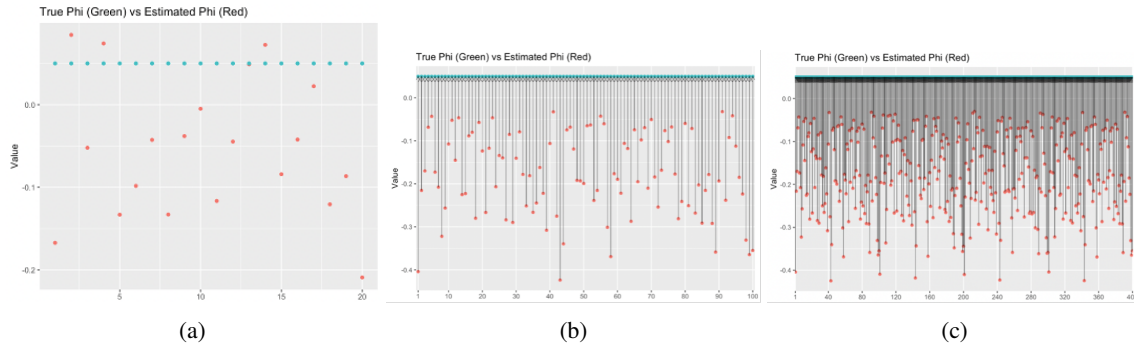


Figure 4: Comparison of true φ_i to estimated $\hat{\varphi}_i$

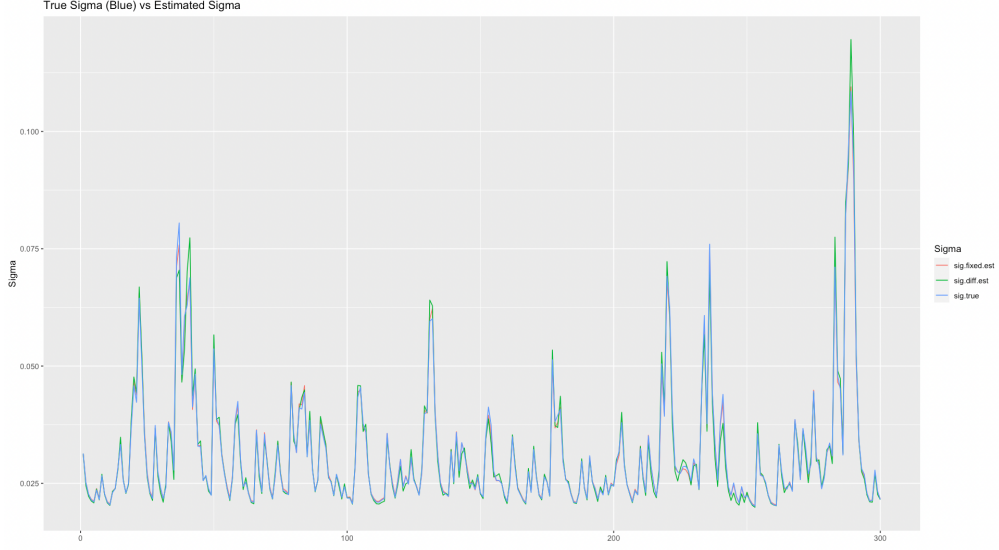


Figure 5: Plots of actual sigma $\sigma_{t|t-1}$ and estimated sigma $\hat{\sigma}_{t|t-1}$

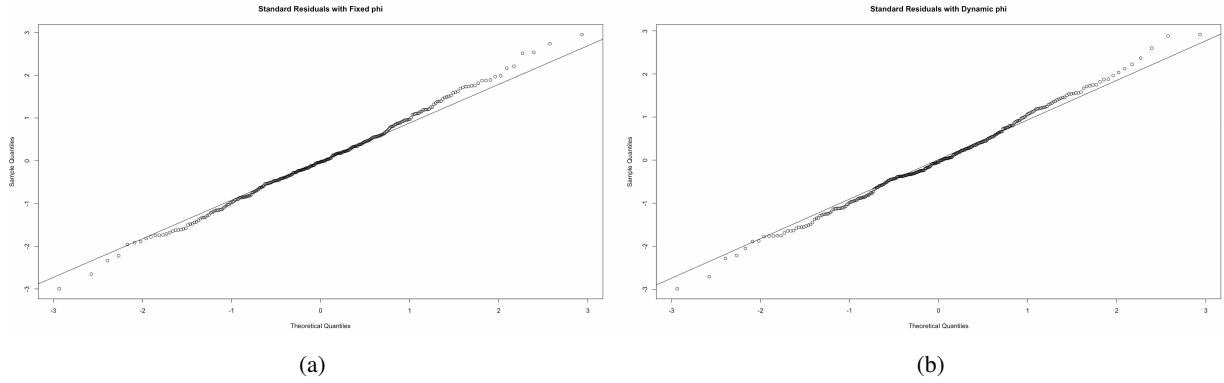


Figure 6: plots of actual residuals ε_t and estimated residuals $\hat{\varepsilon}_t$

4.2 Simulation study II - Modelling with dynamic parameters

In this section of study II, some statistical analysis results are presented to compare modelling performance when φ_i is fixed and dynamic.

To compare estimator $\hat{\sigma}_{t|t-1}$ when φ_i is in different scenarios, it is necessary to plot actual values and estimated values together to study.

Figure 5 demonstrates that the values of two different estimators $\hat{\sigma}_{t|t-1}$ are quite good, because both estimators fit the actual values. While the figure reveals some estimation errors on large $\hat{\sigma}_{t|t-1}$, the estimators do not perform well when estimating large values.

Similarly, the distribution of standardized residuals ε_t can be examined by Q-Q plots. The above Q-Q plots, Figure 6, indicate that both estimators $\hat{\varepsilon}_t$ follow a normal distribution. The data points follow the central line very closely for estimators $\hat{\varepsilon}_t$.

Moreover, the orders of GARCH model are accurately identified as (1, 1). AIC is used to compare GARCH(1, 1) with GARCH(2, 2) to prove the identification method works correctly.

According to AIC, the best-fit model explains the most significant amount of variation using the fewest possible independent variables. Regarding Table 3, it gives apparent results that GARCH(1, 1) is always better than GARCH(2, 2) to fit shared volatility clustering $\hat{\varepsilon}_t$ no matters whether φ_i is fixed to 0.05 or dynamic in range (0.7, 0.9). When only considering model GARCH(1, 1), it performs better when φ_i is dynamic in range (0.7, 0.9).

AIC	GARCH(1, 1)	GARCH(2, 2)
$0.7 < \varphi < 0.09$	-0.6760055	-0.6653040
$\varphi = 0.05$	-0.6710866	-0.6620987

Table 3: Comparison of AIC values between two models when φ in different ranges

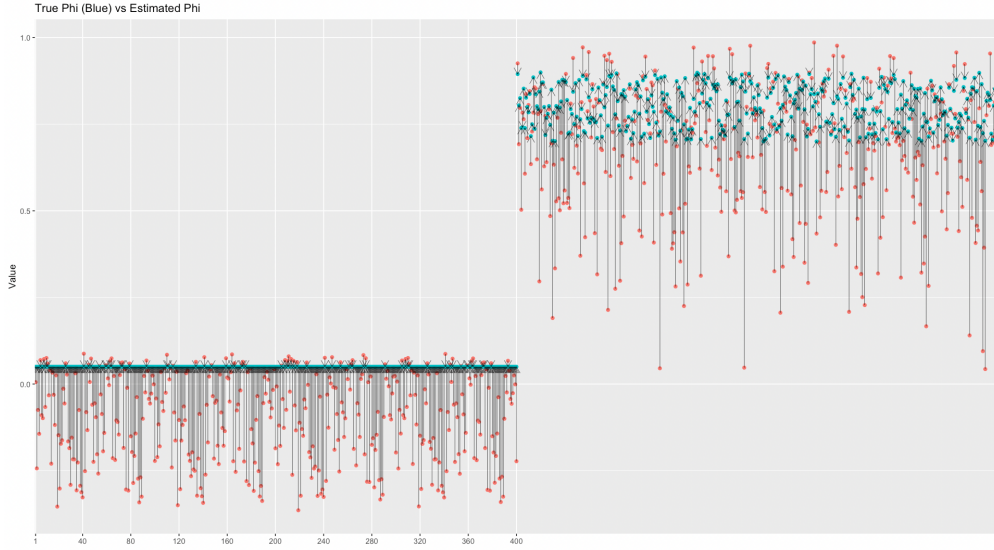


Figure 7: Comparison of true φ_i to estimated $\hat{\varphi}_l$

In terms of the estimator $\hat{\varphi}_l$, the results are presented by a scatter plot.

For each φ_i , the scatter plot can illustrate the distance between the actual value and the estimated value. The scatter plot, Figure 7, indicates the bias of this estimator $\hat{\varphi}_l$ exists when the actual value of φ_i is fixed or dynamic. Therefore, it requires improvement of the analysis methods to achieve better estimation.

4.3 Simulation study III - Dynamic parameters in different ranges

In this section of study III, the outcomes of modelling and parameter estimation illustrate that the improvement of previous statistical methods impact estimation accuracy.

The first parameter to compare is $\sigma_{t|t-1}$ ($\hat{\sigma}_{t|t-1}$). The data set consists of 200 simulated time series with φ_i close to 0.0 and 200 simulated time series with φ_i close to 1.0. After fitting AR models on each series and computing the

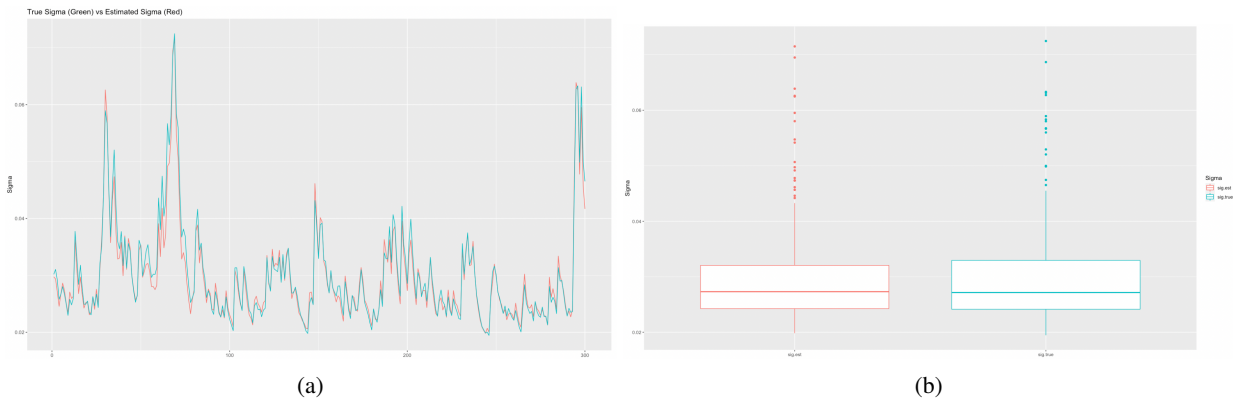


Figure 8: Left plot shows true φ_i and estimated $\hat{\varphi}_l$, right boxplot shows mean and variance of $\hat{\varphi}_l$ and φ_i respectively

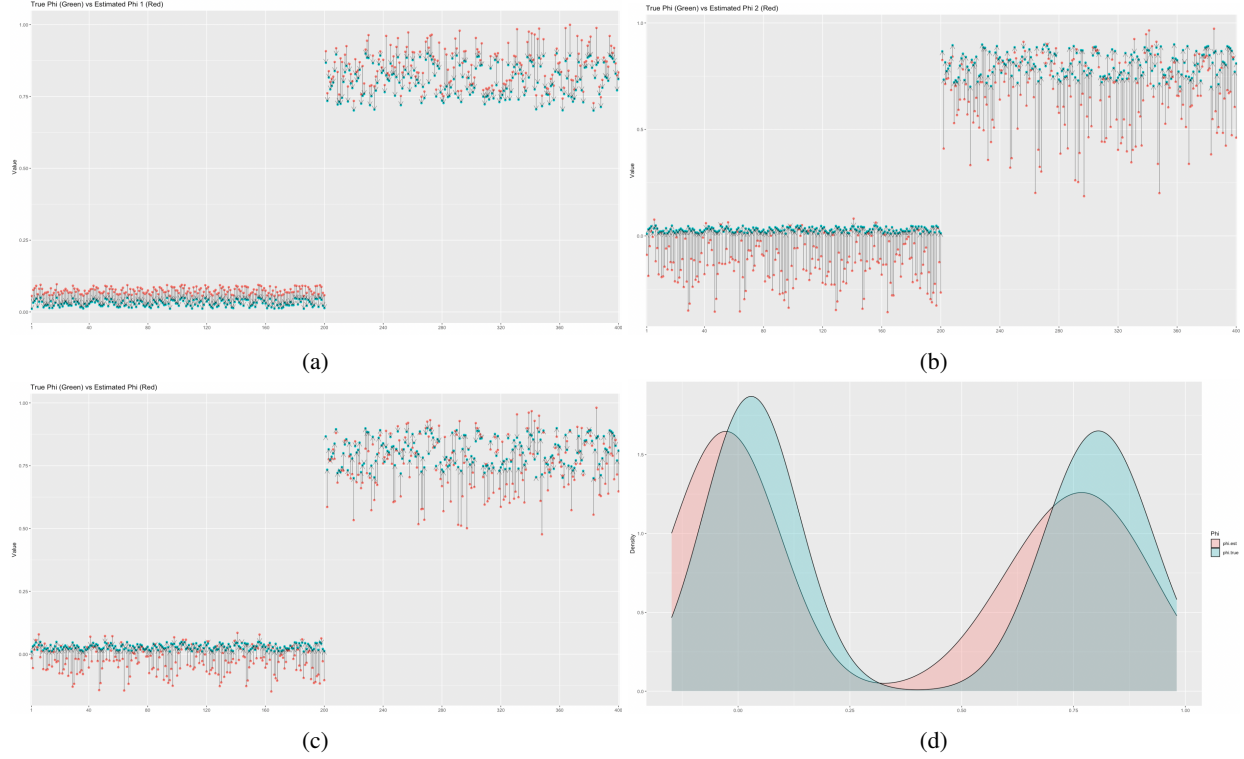


Figure 9: The top left plot shows bias of the first estimator $\hat{\varphi}_{1i}$, the top right plot shows bias of the second estimator $\hat{\varphi}_{2i}$. The bottom left plot indicates more accurate estimator $\hat{\varphi}_l$ after averaging $\hat{\varphi}_{1i}$ and $\hat{\varphi}_{2i}$. The bottom right plot shows density of estimator $\hat{\varphi}_l$ in two ranges (0.01, 0.05) and (0.7, 0.9)

averaged residuals $\bar{\eta}_t$ with weights W_i , the estimator $\hat{\sigma}_{t|t-1}$ is still close to $\sigma_{t|t-1}$. Although Figure 8 displays the bias of estimator $\hat{\sigma}_{t|t-1}$ on local minimum values and local maximum values on the left line plot, the boxplot on the right indicates the mean value of estimator $\hat{\sigma}_{t|t-1}$ is equal to mean of $\sigma_{t|t-1}$. Also, the variance of estimation is approximately equal to 0.00081572.

The estimation of standardized residuals ε_t is good as expected since the Q-Q plot of estimator $\hat{\varepsilon}_t$ follows a normal distribution without many differences from $\hat{\varepsilon}_t$ generated from previous methods. In other words, the estimator $\hat{\varepsilon}_t$ is not impacted by averaging residuals $\{\hat{\eta}_{it}\}$ with weights W_i . This supports the assumption that the improvement of statistical methods reduces the bias of estimator $\hat{\varphi}_l$ without influencing estimator $\hat{\varepsilon}_t$.

The idea of the improved analysis methods is calculating the estimation of φ_i by averaging $\hat{\varphi}_{1i}$ and $\hat{\varphi}_{2i}$. For this reason, the new estimator $\hat{\varphi}_l$ considers outputs from two estimators $\hat{\varphi}_{1i}$ and $\hat{\varphi}_{2i}$ generated from two different steps during modelling.

The first estimator $\hat{\varphi}_{1i}$ is generated with bias after fitting AR model on each series. The top left plot in Figure 9 reveals that most estimation values are smaller than the actual values. Furthermore, the top right plot shows bias when most estimation values are larger than the actual values. Hence, the second estimator $\hat{\varphi}_{2i}$ also generates the bias. Whereas the way of averaging $\hat{\varphi}_{1i}$ and $\hat{\varphi}_{2i}$ reduce the bias of estimator $\hat{\varphi}_l$ remarkably, illustrated by the bottom left plot in Figure 9. It is expected to achieve minimum bias of estimator $\hat{\varphi}_l$ without significantly influencing the accuracy of other estimators $\hat{\sigma}_{t|t-1}$ and $\hat{\varepsilon}_t$.

Table 4 summarises the estimation results of φ_i that are achieved when φ_i is fixed and dynamic in different ranges, (0.01, 0.05) and (0.7, 0.9), with varying sizes of simulated data sets. It demonstrates that the improved method with proposed weights parameter W_i avoids the apparent bias of estimator $\hat{\varphi}_l$ as expected. It is necessary to calculate the estimator $\hat{\varphi}_l$ twice to give the final estimation of φ_i .

4.4 Practice study – Real-world fMRI data

The following steps are performed to model the real-world fMRI data: (1) Identify AR orders \bar{u} of each fMRI series and fit estimated AR (\bar{u}) model to get estimator $\hat{\varphi}_{1i}$ and residuals $\{\hat{\eta}_{it}\}$. (2) Use estimator $\hat{\varphi}_{1i}$ to calculate weights W_i ,

K	$\varphi = 0.05$	$0.01 < \varphi < 0.05$	$0.7 < \varphi < 0.9$	Results
20	0.01736553	-	-	0.01736553
100	0.06222519	-	-	0.06222519
400	0.06175203	-	-	0.06175203
100	-	-	0.03460226	0.03460226
400	-	-	0.0364705	0.0364705
200	-	0.005858768	-	0.01736553
200	-	-	0.009149003	

Table 4: Summary of estimation results for parameter φ_i in different ranges with different sizes of data sets

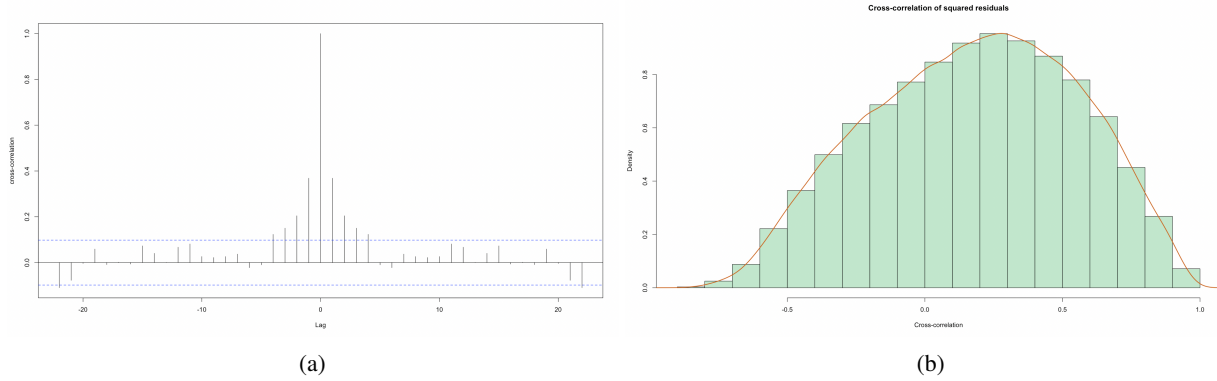


Figure 10: The left plot shows cross-correlation of $\{\hat{\eta}_{it}\}$. The density of cross-correlation on the right plot

then calculate averaged residuals $\bar{\eta}_t$ with the equation: $\bar{\eta}_t = \sum W_i \hat{\eta}_{it}$. (3) Identify GARCH orders (\hat{p}, \hat{q}) on $\bar{\eta}_t$ and fit a GARCH(\hat{p}, \hat{q}) model. (4) Without averaging residuals, fit each residuals η_{it} with GARCH(\hat{p}, \hat{q}) models to get estimator $\hat{\varphi}_{i_old}$ (this is the old analysis method used for estimating φ_i). (5) Remove $\bar{\eta}_t$ from each fMRI series and fit returns with AR(\bar{u}) model to get estimator $\hat{\varphi}_{2i}$. (6) Calculate estimator $\hat{\varphi}_i$ by averaging $\hat{\varphi}_{1i}$ and $\hat{\varphi}_{2i}$. Statically assess GARCH model fitting and compare parameter estimators $\hat{\varphi}_i (= (\hat{\varphi}_{1i} + \hat{\varphi}_{2i})/2)$ to $\hat{\varphi}_{i_old}$.

Subject CC10056: The findings of our study on CC10056 are presented in this section.

It is necessary to justify the GARCH model choice that the volatility is shared over the 400 ROIs. Accordingly, the 400×400 cross-correlation matrix between the squared residuals $\{\hat{\eta}_{it}\}$ is calculated and plotted visually. Figure 10 shows that the distribution of cross-correlation is not centred on zero, instead it is centred on a positive value.

The plot of averaged residuals $\bar{\eta}_t$ clearly reveals volatility clustering. Also, it fails McLeod-Li, so there is evidence of ARCH type behaviour in the model.

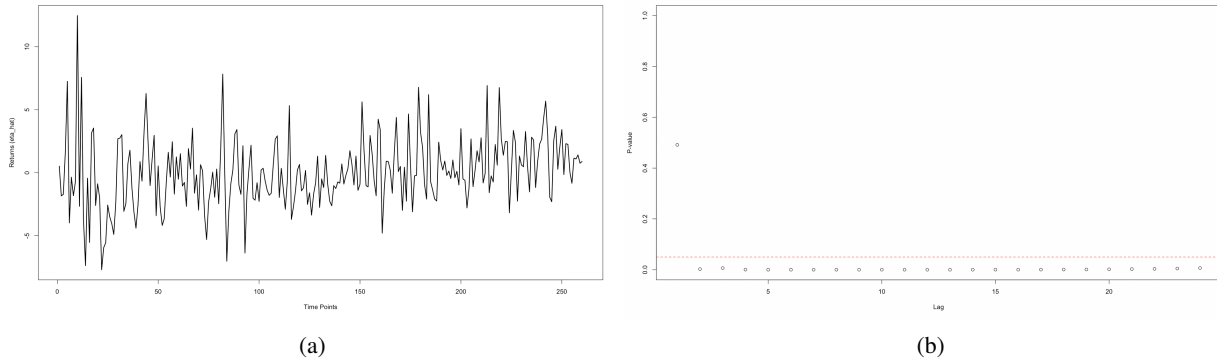


Figure 11: The left plot shows volatility clustering. The McLeod-Li test results on the right

	Estimate	Std. Error	t value	Pr (> t)
omega	0.52535	0.34033	1.544	0.1227
alpha1	0.06399	0.03611	1.772	0.0764
beta1	0.86132	0.06874	12.529	< 2e - 16

Table 5: Summary of estimated coefficients for GARCH model on CC10056 shared residuals

	GARCH(1, 1)	GARCH(2, 2)
AIC	4.834117	4.844648

Table 6: AIC for GARCH(1, 1) and GARCH(2, 2)

The averaged residuals $\bar{\eta}_t$ can be fitted with a GARCH(1, 1) model. The coefficients $\hat{\alpha}_1$ is significant, although $\hat{\beta}_1$ is slightly larger than 0.05 if the confidence interval is considered 0.05.

Another model, GARCH(2, 2), is also fitted on $\bar{\eta}_t$ to compare fitting results to GARCH(1, 1). The AIC indicates that GARCH(1, 1) model is better than GARCH(2, 2) in terms of fitting $\bar{\eta}_t$.

Therefore, the equation of the GARCH model is written as below:

$$\begin{aligned} \bar{\eta}_t &= \sigma_{t|t-1}\varepsilon_t \\ \sigma_{t|t-1}^2 &= 0.52535 + 0.06399\eta_{t-1}^2 + 0.86132\sigma_{t-1|t-2}^2 \\ \varepsilon_t &\sim N(0, 1) \end{aligned} \tag{16}$$

The final line shows the Li-Mak test (Li and Mak, 1994) results, indicating that we successfully modelled out the ARCH behaviour in the series. Equivalently, the Li-Mak test inspects the presence of autocorrelation in their squares, showing a sign that the GARCH model captures all autoregressive conditional heteroskedastic patterns there are.

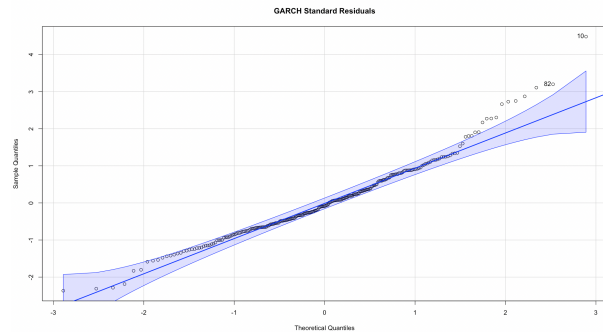
The standard residuals $\hat{\varepsilon}_t$ is examined by a Q-Q plot with the confidence interval of 0.05. It illustrates standardized residuals follow a normal distribution, see Figure 12.

The estimator $\hat{\varphi}_{1i}$, $\hat{\varphi}_{2i}$ and $\hat{\varphi}_{i_old}$ are examined by scatter plots. Since some fMRI series are identified as AR models with orders larger than 2, in this case, only the first two coefficients $\hat{\varphi}_1$ and $\hat{\varphi}_2$ are discussed. To compare the estimator $\hat{\varphi}_i$ (generated from the improved analysis method) to the estimator $\hat{\varphi}_{i_old}$ (generated from old analysis method), a possible method is comparing their standard error returned from modelling. Remember that estimator $\hat{\varphi}_i$ is equal to

Standardised Residuals Tests:

			Statistic	p-Value
Jarque-Bera Test	R	Chi^2	54.01294	1.867395e-12
Shapiro-Wilk Test	R	W	0.9658048	7.309328e-06
Ljung-Box Test	R	Q(10)	21.42225	0.01833419
Ljung-Box Test	R	Q(15)	29.73667	0.01290727
Ljung-Box Test	R	Q(20)	34.85436	0.02089379
Ljung-Box Test	R^2	Q(10)	8.39217	0.5905882
Ljung-Box Test	R^2	Q(15)	9.261582	0.8634477
Ljung-Box Test	R^2	Q(20)	9.682714	0.9735671
LM Arch Test	R	TR^2	4.56039	0.971077

(a)



(b)

Figure 12: The left plot shows tests for ARCH/GARCH behaviour in standardized residuals The right Q-Q plot of standardized residuals reveals a normal distribution

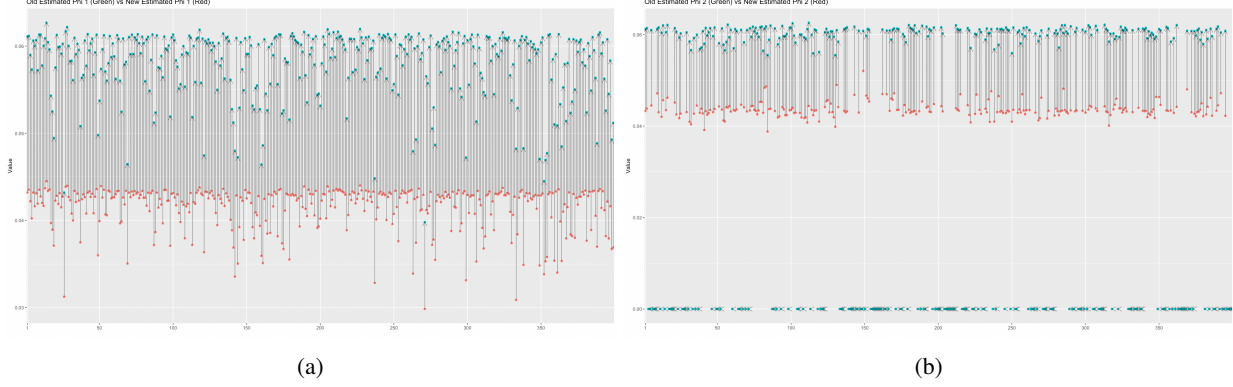


Figure 13: The left plot standard error of estimation of the first coefficient φ_1 . The right plot standard error of estimation of the second coefficient φ_2

	Estimate	Std. Error	t value	Pr (> t)
omega	$6.090e - 01$	$4.849e - 01$	1.256	0.20910
alpha1	$1.000e - 08$	<i>NaN</i>	<i>NaN</i>	<i>NaN</i>
alpha2	$5.550e - 02$	<i>NaN</i>	<i>NaN</i>	<i>NaN</i>
beta1	$6.855e - 01$	$2.094e - 01$	3.273	0.00106

Table 7: Summary of estimated coefficients for GARCH(2, 1) model on CC10045 shared residuals

$(\hat{\varphi}_{1i} + \hat{\varphi}_{2i})/2$, thus the standard error of $\hat{\varphi}_i$ is given by the following equation:

$$\begin{aligned}
 SE(\hat{\varphi}_i) &= \sqrt{\text{Var}(\hat{\varphi}_i)} \\
 &= \sqrt{\frac{1}{4} \text{Var}(\hat{\varphi}_{1i} + \hat{\varphi}_{2i})} \\
 &= \frac{1}{2} \sqrt{\text{Var}(\hat{\varphi}_{1i}) + \text{Var}(\hat{\varphi}_{2i})}
 \end{aligned} \tag{17}$$

The variance of $\hat{\varphi}_{1i}$ and $\hat{\varphi}_{2i}$ can be calculated by squaring off the standard error of $\hat{\varphi}_{1i}$ and $\hat{\varphi}_{2i}$ returned by AR model. Using visualization tools is the straight method to compare two estimators for the first coefficient φ_1 and the second coefficient φ_2 . The scatter plots, Figure 13 reveal that the standard error of the estimator $\hat{\varphi}_i$ is smaller than the standard error of old estimator $\hat{\varphi}_{i_old}$ if the coefficients $\hat{\varphi}_i$ and $\hat{\varphi}_{i_old}$ are neither equal to zero.

When averaged residuals $\bar{\eta}_t$ and conditional variance $\hat{\sigma}_{t|t-1}$ are displayed together, Figure 14a and 14b, the GARCH(1, 1) model tries to capture volatility. It mainly evidences that the model tracks some significant volatility clusters well. Moreover, Figure 14d, the ACF plot of squared $\bar{\eta}_t$ shows high cross-correlation, and the ACF of standardized residuals $\hat{\varepsilon}_t$, Figure 14f, does not display many autocorrelations at low lags.

Subject CC10045 The findings of our study on CC10045 are presented in this section.

The plot of averaged residuals $\bar{\eta}_t$ does not show much high volatility. Instead, it shows volatility clustering at the last few time points. Also, it passed McLeod-Li test, so the null hypothesis cannot be rejected. Thus there is no evidence of ARCH type behaviour in the model, see Figure 15.

It is still necessary to fit the averaged residuals $\bar{\eta}_t$ with a GARCH model to assess its parameters statistically. The orders of GARCH are identified as (2, 1). A GARCH(2, 1) model is fitted. The coefficients $\hat{\beta}_1$ is significant if the confidence interval is considered 0.05. But $\hat{\alpha}_1$ and $\hat{\alpha}_2$ have NaN p-values, which means their fitted probabilities are 0 or 1. The p-values suggest that only $\hat{\beta}_1$ is the significant coefficient required. Nevertheless, building any GARCH or ARCH model with coefficients $\hat{\beta}_1$ only is impossible, see Table 7. Despite this, other models, GARCH(1, 1) and GARCH(2, 2), are still fitted on $\bar{\eta}_t$ to compare fitting results to GARCH(2, 1). The AIC, in Table 8, indicates that GARCH(2, 1) model is still better than others in terms of fitting $\bar{\eta}_t$.

When squared residuals $\bar{\eta}_t^2$ and conditional variance $\hat{\sigma}_{t|t-1}$ are plotted together, Figure 16a and 16b, it indicates that the model fitting fails a test for normality. The GARCH(2, 1) model cannot capture any volatility. The ACF plot of squared

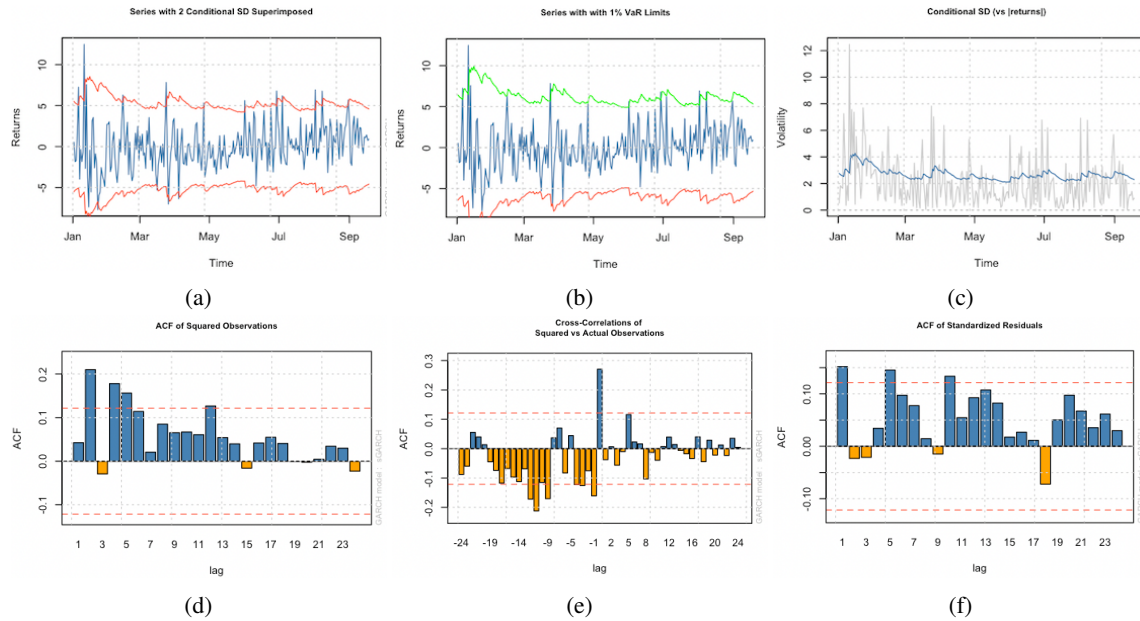


Figure 14: (a) and (b) show the residuals $\hat{\eta}_t$ against conditional variance. (c) plots conditional standard deviation against residuals $\hat{\eta}_t$. (d) ACF of squared $\hat{\eta}_t$. (e) Cross-correlation of $\hat{\eta}_t$ and squared $\hat{\eta}_t$. (f) ACF of standardized residuals $\hat{\epsilon}_t$

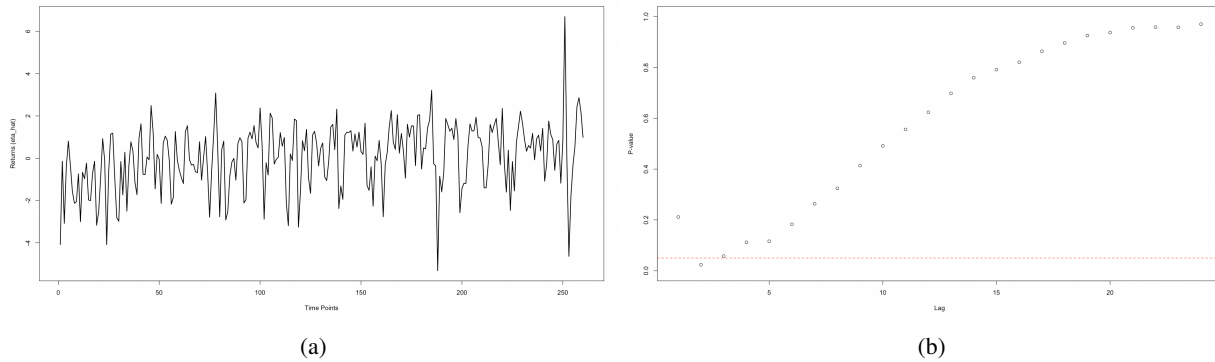


Figure 15: The left plot shows volatility clustering. The McLeod-Li test results on the right

	GARCH(1, 1)	GARCH(2, 1)	GARCH(2, 2)
AIC	3.733134	3.731101	3.738661

Table 8: AIC for GARCH(1, 1), GARCH(2, 1), and GARCH(2, 2)

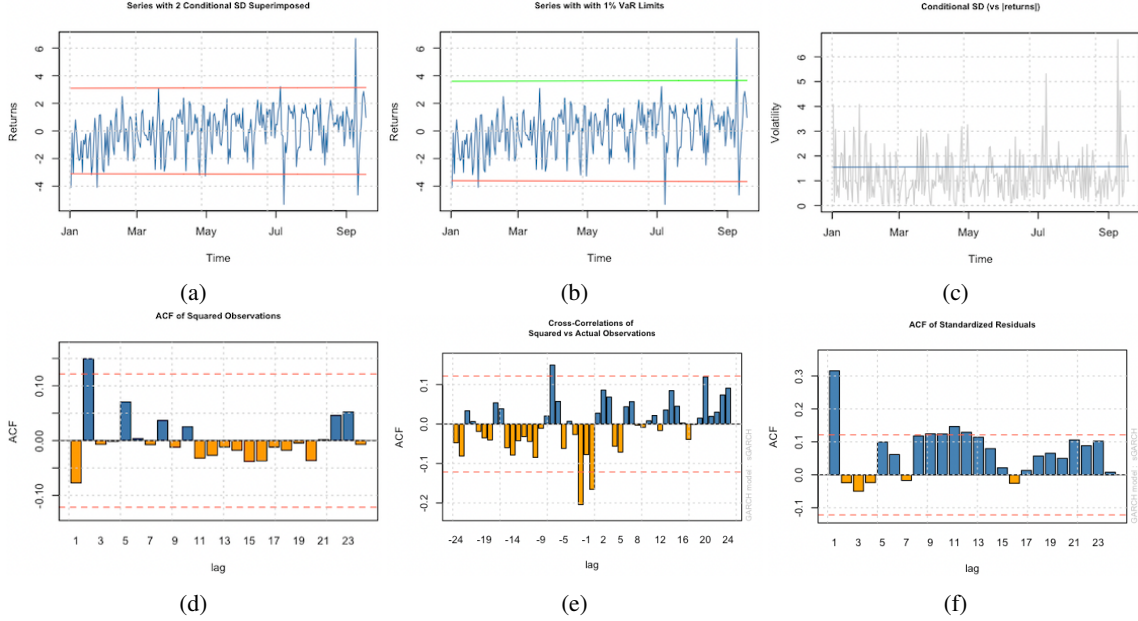


Figure 16: (a) and (b) show the residuals $\hat{\eta}_t$ against conditional variance. (c) plots conditional standard deviation against residuals $\hat{\eta}_t$. (d) ACF of squared $\hat{\eta}_t$. (e) Cross-correlation of $\hat{\eta}_t$ and squared $\hat{\eta}_t$. (f) ACF of standardized residuals $\hat{\epsilon}_t$

$\hat{\eta}_t$, Figure 16d, only shows non-null autocorrelations at lag 2. Figure 16f, the plot of standardized residuals $\hat{\epsilon}_t$ illustrates non-null autocorrelations at low lags, so it does not follow a normal distribution.

It is not necessary to compare the estimator $\hat{\varphi}_i$ (or $\hat{\varphi}_{1i}, \hat{\varphi}_{2i}$) to $\hat{\varphi}_{i_old}$. This is because the squared residual $\hat{\eta}_t$ does not have much high volatility, and fitting the GARCH model is not a suitable modelling method. Instead, most fMRI series are identified as AR models with orders 1, 2 and 3. It implies that the subject CC10045 can be modelled with multiple AR(\hat{u}_i) models.

5 Conclusions

This paper evaluates a novel aspect of adapting an approach to handle fMRI time series data CC10045 and CC10056 for infants because infant data have “innovations” (sudden movements) associated with them, which results in jumps in the time series data. The proposed approach tries to model these jumps as shared volatility clustering across the time series (brain regions). The shared volatility clustering is modelled as GARCH models configured with the normal distribution, and the superior GARCH model is chosen based on which model achieves the smallest AIC. Each series is modelled as independent AR models. The estimations of model parameters are examined by the standard error, MSE and graphical examinations. The performance of modelling is evaluated by the performance measures MSE.

All GARCH models in this project are configured with the normal distribution. The simulation work proves that multiple dependent AR(1) + GARCH(1, 1) time series data have shared volatility modelled successfully. The Q-Q plot of the standardized residuals shows that our prespecified distribution assumption ($\sim N(0, 1)$) was correct. The graphical examination of conditional variance shows that GARCH model tends to estimate the shared volatility clustering. The parameters of AR parts are underestimated when shared volatility clustering is not weighted. After calculating the weighted shared volatility clustering by AR coefficients and averaging coefficient estimators, the estimation of AR parameters has increased accuracy. Equivalently, the MSE of parameter estimators are heavily reduced. The real-world fMRI data CC10056 with many movements is identified as multiple AR models with different orders in the range [1, 5] and a GARCH(1, 1) model. The GARCH(1, 1) model tries to capture the shared volatility clustering. Also, the graphical examination of AR coefficients shows that they are estimated accurately. The real-world fMRI data CC10045 is identified as multiple AR models. However, the share volatility clustering cannot be modelled by a GARCH model. It does not reveal conditional heteroscedasticity, as it does not pass statistical tests. Moreover, the best model, GARCH(2, 1) chosen, cannot capture shared volatility clustering.

The results, therefore, imply that the weighted shared volatility improves the modelling performance of the GARCH models when handling fMRI time series data for infants with many movements across brain regions. Furthermore,

averaging the AR coefficient estimators is a vital characteristic to account for when modelling multiple dependent time series.

References

- P. A. Moran. Hypothesis Testing in Time Series Analysis. *Royal Statistical Society. Journal. Series A: General*, 114(4): 579–579, 12 2018. ISSN 0035-9238. doi:10.2307/2981095. URL <https://doi.org/10.2307/2981095>.
- Judith Corbyn. Time Series Analysis with Applications in R, 2nd edn. *Journal of the Royal Statistical Society Series A: Statistics in Society*, 174(2):507–507, 03 2011. ISSN 0964-1998. doi:10.1111/j.1467-985X.2010.00681_4.x. URL https://doi.org/10.1111/j.1467-985X.2010.00681_4.x.
- Tim Bollerslev. Generalized autoregressive conditional heteroskedasticity. *Journal of Econometrics*, 31(3):307–327, 1986. ISSN 0304-4076. doi:https://doi.org/10.1016/0304-4076(86)90063-1. URL <https://www.sciencedirect.com/science/article/pii/0304407686900631>.
- Mehdi Zolfaghari and Samad Gholami. A hybrid approach of adaptive wavelet transform, long short-term memory and arima-garch family models for the stock index prediction. *Expert Systems with Applications*, 182:115149, 2021. ISSN 0957-4174. doi:https://doi.org/10.1016/j.eswa.2021.115149. URL <https://www.sciencedirect.com/science/article/pii/S095741742100590X>.
- Xianfu Lin and Yuzhang Huang. Short-Term High-Speed traffic flow prediction based on ARIMA-GARCH-M model. *Wireless Personal Communications*, 117(4):3421–3430, April 2021.
- Takuya Ito, Luke J. Hearne, and Michael W. Cole. A cortical hierarchy of localized and distributed processes revealed via dissociation of task activations, connectivity changes, and intrinsic timescales. *NeuroImage*, 221:117141, 2020. ISSN 1053-8119. doi:https://doi.org/10.1016/j.neuroimage.2020.117141. URL <https://www.sciencedirect.com/science/article/pii/S1053811920306273>.
- Patrick L. Purdon, Victor Solo, Robert M. Weisskoff, and Emery N. Brown. Locally regularized spatiotemporal modeling and model comparison for functional mri. *NeuroImage*, 14(4):912–923, 2001. ISSN 1053-8119. doi:https://doi.org/10.1006/nimg.2001.0870. URL <https://www.sciencedirect.com/science/article/pii/S1053811901908705>.
- Cheryl L Grady and Douglas D Garrett. Understanding variability in the BOLD signal and why it matters for aging. *Brain Imaging Behav*, 8(2):274–283, June 2014.
- Nikos K Logothetis, Jon Pauls, Mark Augath, Torsten Trinath, and Axel Oeltermann. Neurophysiological investigation of the basis of the fMRI signal. *Nature*, 412(6843):150–157, July 2001.
- Nikos K Logothetis. The neural basis of the blood-oxygen-level-dependent functional magnetic resonance imaging signal. *Philos Trans R Soc Lond B Biol Sci*, 357(1424):1003–1037, August 2002.
- N Kanwisher, J McDermott, and M M Chun. The fusiform face area: a module in human extrastriate cortex specialized for face perception. *J Neurosci*, 17(11):4302–4311, June 1997.
- J V Haxby, M I Gobbini, M L Furey, A Ishai, J L Schouten, and P Pietrini. Distributed and overlapping representations of faces and objects in ventral temporal cortex. *Science*, 293(5539):2425–2430, September 2001.
- Koene R.A. Van Dijk, Mert R. Sabuncu, and Randy L. Buckner. The influence of head motion on intrinsic functional connectivity mri. *NeuroImage*, 59(1):431–438, 2012. ISSN 1053-8119. doi:https://doi.org/10.1016/j.neuroimage.2011.07.044. URL <https://www.sciencedirect.com/science/article/pii/S1053811911008214>. Neuroergonomics: The human brain in action and at work.
- A. I. McLeod and W. K. Li. Diagnostic checking arma time series models using squared-residual autocorrelations. *Journal of Time Series Analysis*, 4(4):269–273, 1983. doi:https://doi.org/10.1111/j.1467-9892.1983.tb00373.x. URL <https://onlinelibrary.wiley.com/doi/abs/10.1111/j.1467-9892.1983.tb00373.x>.
- Robert F. Engle. Autoregressive conditional heteroscedasticity with estimates of the variance of united kingdom inflation. *Econometrica*, 50(4):987–1007, 1982. ISSN 00129682, 14680262. URL <http://www.jstor.org/stable/1912773>.
- G. M. LJUNG and G. E. P. BOX. On a measure of lack of fit in time series models. *Biometrika*, 65(2):297–303, 08 1978. ISSN 0006-3444. doi:10.1093/biomet/65.2.297. URL <https://doi.org/10.1093/biomet/65.2.297>.
- Nagaraj Naik, Biju R Mohan, and Rajat Aayush Jha. Garch-model identification based on performance of information criteria. *Procedia Computer Science*, 171:1935–1942, 2020. ISSN 1877-0509. doi:https://doi.org/10.1016/j.procs.2020.04.207. URL <https://www.sciencedirect.com/science/article/pii/S1877050920311893>. Third International Conference on Computing and Network Communications (CoCoNet’19).

M. B. WILK and R. GNANADESIKAN. Probability plotting methods for the analysis for the analysis of data. *Biometrika*, 55(1):1–17, 03 1968. ISSN 0006-3444. doi:10.1093/biomet/55.1.1. URL <https://doi.org/10.1093/biomet/55.1.1>.